Pergamon

*Pattern Recognition*, Vol. 27, No. 3, pp. 339–349, 1994
Elsevier Science Ltd
Pattern Recognition Society

0031-3203/94 $6.00 + .00

# CAN THE FRACTAL DIMENSION OF IMAGES BE MEASURED?

QIAN HUANG, JACOB R. LORCH and RICHARD C. DUBES
Department of Computer Science, Michigan State University, East Lansing, MI 48823-1027, U.S.A.

(*Received* 16 *December* 1993; *in revised form* 5 *October* 1993; *received for publication* 13 *October* 1993)

**Abstract**—Fractal dimension is a popular parameter for explaining certain phenomena and for describing natural textures. The problem of estimating the fractal dimension of a profile or an image is more difficult and devious than theory suggests. This paper studies the accuracy and robustness of two common estimators of fractal dimension (box counting and the variation method) using two types of data (Brownian and Takagi). Poor results are demonstrated from applying theory directly, called naive estimation. Data is then interpreted in the most optimistic way possible by matching the estimator to the known fractal dimension. Experiments quantify the effects of resolution, or fineness of sampling, and quantization, or rounding of sampled values. Increasing resolution enhances the estimators when true dimension, $D$, is large, but may, possibly due to quantization effect, degrade estimators when $D$ is small. Quantization simply causes shifts in estimates. The results suggest that one should not place much reliance in the absolute value of a fractal estimate, but that the estimates do vary monotonically with $D$ and might be useful descriptors in tasks such as image segmentation and description.

Fractal dimension    Image description    Estimation of dimension    Brownian surface

## 1. INTRODUCTION

Fractal dimension has become ubiquitous in science ever since Mandelbrot's provocative book appeared[1] and the fantastic images of fractal sets became popular.[2] In addition to being a source of pretty pictures, fractal geometry has been used to characterize the behavior of chaotic systems,[3] to reveal new insights into mathematics,[4] to define models of natural objects,[1] and to suggest models in the life sciences.[5] Fractals have been applied to the general area of image analysis as a means for compressing images,[4] as a vehicle for segmenting images,[6] and as a descriptor of radiographic images.[7] The list of applications could continue for several pages.

Many applications of fractal concepts rely on the ability to accurately estimate the fractal dimensions of objects from samples, especially when chaotic, nonlinear systems are being characterized or when images are being compressed. The issues of resolution and quantization are continually encountered when trying to validate and compare various algorithms for estimating the fractal dimension of images. Each algorithm for estimating fractal dimension involves parameters which must be chosen heuristically but which can have a dramatic effect on the results. Little hard evidence exists to quantify the influences of these factors on the accuracy of estimates. In our experience, simply programming an estimator from theory does not usually provide good estimates. The repeated failure of all estimators of fractal dimension on certain images which were supposed to be pure fractal images led to the question that became the title of this paper and to the following related questions. Are there subtle, but inherent difficulties that will always frustrate the estimation of fractal dimension? Are there enough practical difficulties in this estimation problem to render it unsolvable in practice? We report on some experiments that contribute to answering such questions with emphasis on resolution and quantization.

This paper focuses on fractal images and fractal profiles. Kube and Pentland[8,9] have studied the conditions under which imaging produces a fractal surface. Certain types of medical images are good candidates for fractal description because of the way in which the images are collected.[10] Fractal dimension has served as the vehicle for segmenting an image,[6] which means separating the image into its constituent parts and labeling them. Estimates of fractal dimension alone are not normally sufficient to segment an image; additional features such as lacunarities, signatures, variances, and non-fractal features need to be added to segment certain types of images, such as images containing natural textures.[11–15]

The inaccurate estimation of fractal dimension does not preclude an estimator from being an effective agent in image segmentation. The estimator should, however, vary monotonically with true fractal dimension so that one can treat an estimator of fractal dimension as a feature in a segmentation process. As long as the feature is able to separate the parts of an image, the accuracy with which some physical or mathematical characteristic is being measured may be of secondary interest. Our experiments are designed to test the accuracy of fractal estimators, not to assess their efficacy in segmenting images. It is important to understand which factors contribute to inaccuracy if fractal dimension is to be used most effectively.

## 2. FRACTAL DIMENSION

The word *fractal* has many uses. We begin with the notion that a fractal is a set having non-integer dimension. Theoretically, a fractal exhibits the same characteristics at all levels of resolution. With the proper normalization, one cannot determine the resolution at which the fractal is being observed. The fractals discussed in this paper either have dimension between 1 and 2 (profiles) or between 2 and 3 (surfaces). Profiles are observed as samples of a time series. Surfaces are observed as samples of a digital intensity image defined on a square. The higher the dimension, the more the fractal surface "fills" the underlying space and the "rougher" the surface appears. The estimators discussed in this paper view fractal dimension as a global descriptor of data and work only with sets having a single fractal dimension. Some recent works[16,17] regard fractal dimension as a local descriptor that varies over the image, and estimate fractal dimension with a bank of Gabor filters or with wavelet transformations. Multifractals, or sets involving more than one fractal dimension, are well documented.[18] Such a local, continuously varying fractal dimension is very different from the fractal dimension examined in this paper.

Although the mathematical basis for fractals is well known,[19] the precise relationship between an estimator of fractal dimension and a mathematical concept of dimension, such as Hausdorff–Besikovitch dimension or Minkowski–Bouligand dimension[20] is known only under infinite resolution. Several types of fractal dimension have been mentioned in the literature. Conditions under which the various concepts of fractal dimension are equivalent and the exact connection between definitions of fractal dimension and Hausdorff–Besikovitch dimension are never clear in practice. For example, a fractal has been described as a set whose Hausdorff–Besikovitch dimension exceeds its topological dimension. Another source of confusion is the tendency to define fractal dimension as the quantity being computed by an algorithm, so that various algorithms for fractal dimension may not all be estimating the same quantity. We use the term *fractal dimension* in a generic sense.

This paper concentrates on two estimators of fractal dimension which are based on different fractal characteristics. Test images and profiles having known dimension are generated and two types of results are reported. Naive estimators are based on theoretical considerations alone, as one would do on first encountering the algorithms. Some "optimistic" results are then generated in which the parameters of the estimator are intentionally adjusted to match the known fractal dimension. These two sets of results exhibit the extremes of accuracy and show how initial conditions and parameters can have overwhelming influences on the estimators. The disappointing results achieved by naive estimators motivates the discussion of resolution and quantization as factors which may explain the poor results.

## 3. ESTIMATORS OF FRACTAL DIMENSION

The fractal nature of a set is exhibited in many characteristics of the set, such as length, volume, information, correlations, power spectra, and distance distributions. Theiler[18] and Dubuc *et al.*[20,21] review most of the estimators of fractal dimension proposed in the literature. Underlying mathematical issues in the estimation of fractal dimension have recently been addressed.[22–25] We chose two common estimators of fractal dimension and characterized their behavior in terms of resolution and quantization. To strip away as many sources of confusion as possible, we worked with profiles and images that are "known" to be fractals. A digital image is a set of samples of light intensity taken on an $N \times N$ grid covering the image. A digital profile is a set of $N$ regularly-spaced samples of a time function. Estimators for the fractal dimensions of images are defined in this section. Analogous estimators are used for profiles.

### 3.1. *Box counting*

The box counting estimator of fractal dimension is based on the fact that the number of cubes having side length $L$ needed to cover a fractal surface varies as $L^{-D}$ where $D$ is the fractal dimension that is to be estimated. The box counting algorithm tessellates the cube containing the fractal into boxes, or small cubes, having side length $L$. The number of boxes containing at least one sample of light intensity is denoted by $M(L)$. If the surface being sampled is a fractal surface, then $M(L)$ should be proportional to $L^{-D}$. Plotting the negative log of $M(L)$ against the log of $L$ produces a curve whose slope estimates $D$.

We employ the "fast" box counting method of Liebovitch and Toth[26] to estimate fractal dimension. The side length of the box, $L$, is varied as $2^k$ for $1 \le k \le K$ where $N = 2^K$. This method represents each point on the fractal as a concatenated integer and sorts the set of concatenated integers only once. The values of $M(L)$ are then computed by masking this sorted list. The log–log plot defined above has $K$ points and a straight line is fitted to these points to minimize squared error. The first few and last few values of $k$ may not contain any valuable information. When $k = 1$, $L = 2$ and the boxes are so small that $M(L)$ is limited by the number of samples. When $k = K$, there is only one box, which must certainly be filled. Liebovitch and Toth suggest ignoring values of $k$ for which $M(2^k) < N^2/5$ and ignoring the two largest values $k = K$ and $k = K - 1$. We have found these limits to be too restrictive in image processing.

Voss[27] and Keller *et al.*[12] refer to box counting as the process of centering a box on each sample point for the purpose of estimating the probability that $m$ points lie in the box. The expected number of points in a box is related to fractal dimension. Preliminary investigations suggested that the "fast" box counting method estimated fractal dimension more accurately

DIMENSION

exhibited in many
gth, volume, infor-
., and distance dis-
et al.[20,21] review
mension proposed
natical issues in the
ave recently been
mmon estimators
zed their behavior
ion. To strip away
ssible, we worked
own" to be fractals.
of light intensity
e image. A digital
samples of a time
nensions of images
ous estimators are

actal dimension is
f cubes having side
rface varies as $L^{-D}$
t is to be estimated.
ates the cube con-
nall cubes, having
containing at least
ted by $M(L)$. If the
surface, then $M(L)$
otting the negative
produces a curve

nting method of
fractal dimension.
as $2^k$ for $1 \le k \le K$
nts each point on
r and sorts the set
The values of $M(L)$
is sorted list. The
oints and a straight
nize squared error.
k may not contain
$= 1$, $L = 2$ and the
ted by the number
nly one box, which
and Toth suggest
$< N^2/5$ and ignor-
nd $k = K - 1$. We
estrictive in image

to box counting as
each sample point
probability that $m$
number of points
nsion. Preliminary
ast" box counting
n more accurately

than the Voss–Keller method, which motivated our use of the "fast" box counting algorithm.

### 3.2. *The variation method*

Dubuc *et al.*[20,21] found that analyzing the variation of a fractal surface within small boxes as a function of the box size produced good estimates of fractal dimension. Define the ε-oscillation of a surface function $f$, representing intensity, at point $(x, y)$ in a unit cube to be the difference between the two extreme values of $f$ in an ε-neighborhood of $(x, y)$:

$$v(x, y, \varepsilon) = \sup |f(x_1, y_1) - f(x_2, y_2)|$$

where the supremum is taken over all pairs $(x_1, y_1)$, $(x_2, y_2)$ for which

$$\max\{|x - x_1|, |x - x_2|, |y - y_1|, |y - y_2|\} \le \varepsilon.$$

The volume, or total variation, is defined as

$$V(\varepsilon, f) = \int_0^1\int_0^1 v(x, y, \varepsilon)\,dx\,dy.$$

The fractal dimension $D$ can be shown to satisfy

$$D = \lim_{\varepsilon \to 0}\left(3 - \frac{\log V(\varepsilon, f)}{\log \varepsilon}\right).$$

That is, the estimate of $D$ is 3 minus the slope of the plot of $\log V(\varepsilon_n, f)$ vs. $\log \varepsilon_n$.

Parameter ε is the size of a covering element that defines a box for calculating local oscillations. Following Dubuc *et al.*,[21] function $f(x, y)$ is continuous and defined for all $x$ and $y$ such that $0 \le x \le 1$, $0 \le y \le 1$. Suppose that $f$ is sampled on an $N \times N$ grid. Then the digitized data is defined by $f(i/N, j/N)$ for all $i, j \in \{1, 2, \ldots, N\}$. To approximate the oscillation on this digitized array, these $N \times N$ points are grouped into $R^2$ bins, where $R$ is an integer. The values of ε are

$$\varepsilon_n = k_n/R, \quad n = n_{\min}, \ldots, n_{\max}$$

where $\{k_n\}$ is an increasing sequence of integers, such that

$$k_i = n_i, \quad k_i \le 2 \times k_{i-1}.$$

In our experiment, we chose $R = N$, $n_{\min} = 2$, $n_{\max} = N/2$, and $k_i = k_{i-1} + 1$. Therefore, we used $2/N \le \varepsilon_n \le 1/2$ in plotting the log–log curves. The portion of the log–log plot to which a straight line is fitted must be chosen heuristically. Dubuc *et al.*[20,21] used the heuristic of "best fit" as the criterion in optimizing the portion to be fitted. To serve the goal of this study, we implemented two versions of the variation method, one that uses a fixed portion of the log–log plot in estimation (discussed in Section 5.1) and the other that has the mechanism to optimize the portion of the log–log plot to be fitted according to some criterion (discussed in Section 5.2).

## 4. GENERATION OF FRACTAL IMAGES

Our goal is to examine the accuracy of estimators for fractal dimension so we use only images and profiles having known fractal dimensions. Two algorithms for realizing $N \times N$ fractal images of dimension $D$ are now described. We take $N$ to be a power of 2 and take the range of light intensity to be the integers from 0 to 255. All images are enclosed in rectangular prisms of size $N \times N \times 256$ where $N$ has a value of 64, 128, 256 or 512, depending on the experiment. A Takagi surface, employed by Dubuc *et al.*,[21] is a deterministic function generated in the unit cube and scaled to the appropriate size. The Takagi generator involves no random numbers, so there is only one surface of each size. Samples of the surface at the $N^2$ pixel locations are scaled to integers from 0 to 255. A Takagi surface has planes of symmetry which separate the image into $n \times n$ subplanes, for $n$ a power of 2. This might bias estimators which use windows that line up with these planes of symmetry. Examples of Takagi surfaces are given in Fig. 1.

The midpoint displacement algorithm[28] (pages 96–101), approximates a Brownian surface, or image, by successive refinements in resolution. Brownian profiles were also generated by this method. Random displacements are added during the process, so that the actual image obtained depends on the seed of a random number generator as well as on the fractal dimension. Examples, of Brownian surfaces are shown in Fig. 2.

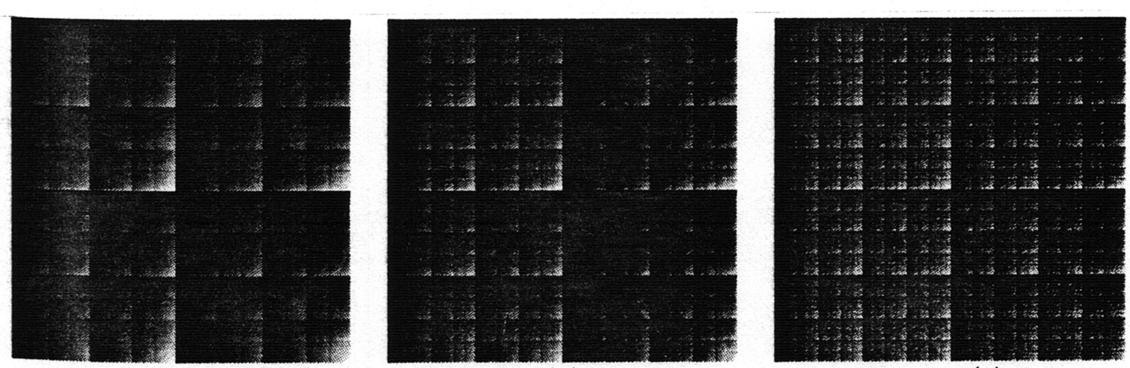

(a) (b) (c)

Fig. 1. Examples of Takagi surfaces: (a) $D = 2.1$; (b) $D = 2.5$; (c) $D = 2.9$.

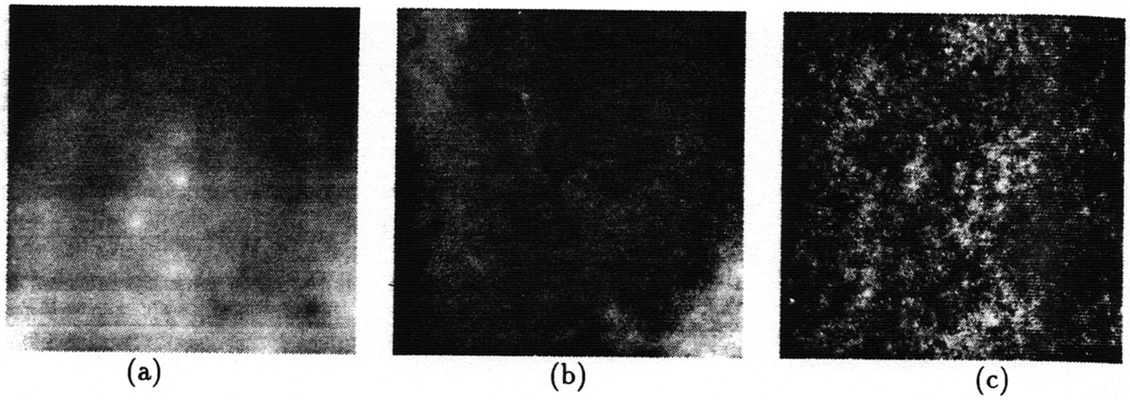

Fig. 2. Examples of Brownian surfaces: (a) $D = 2.1$; (b) $D = 2.5$; (c) $D = 2.9$.

Evaluating the performance of an estimator of fractal dimension requires that these two algorithms do, indeed produce images with the given dimension. These algorithms are popular sources of images in the literature and we have no better alternatives. However, the resolution of such images is inherently limited. A surface with dimension close to 3 is supposed to fill the three-dimensional cube, so the surface must be highly convoluted at all resolutions. An image samples the real surface on a grid and it is not obvious that surfaces with dimension close to 3 can ever be sampled finely enough to capture the true essence of a three-dimensional surface.

## 5. EXPERIMENTS IN ESTIMATING FRACTAL DIMENSION

This section reports the results of experiments in which fractal dimension was estimated from profiles and images under controlled conditions by the variation and box counting methods. Ideally, the log–log plots for the variation and box counting methods defined in Section 3 lie along perfectly straight lines. The finiteness of the data ensures that the plots do not define perfectly straight lines, so one must fit a straight line to some portion of the log–log plot. In box counting, the estimate of fractal dimension is the slope of the fitted straight line itself; in the variation method, the estimate is 3 minus the slope.

To which portion of the log–log plot should the straight line be fitted? A "naive" estimator simply uses a fixed portion of the points on the log–log plot and fits a least-squares straight line to these chosen points. With the variation method, for instance, we use all the points of the log–log data. With box counting, the last point is not used. Thus, the "naive" estimators described in Section 5.1 implement straightforward interpretations of the theory. Experiments with *optimistic* "estimators" in Section 5.2 intentionally try to achieve the best results by choosing the portion of each log–log curve whose slope provides the closest estimate to the known fractal dimension. Such an "optimization" scheme does not inspect the log–log plot to find the most linear portion of the data, an optimization strategy adopted by other researchers in the literature,[20,21] because a best fit does not necessarily guarantee a best estimate.

### 5.1. *Naive estimators*

Test data for the first experiment came from two sources. Brownian profiles having 512 points were generated with true dimensions from 1.1 to 1.9 in steps of 0.1. Brownian images were generated on a 256 × 256 grid with 256 gray levels. The fractal dimension varied from 2.1 to 2.9 in steps of 0.1. Takagi surfaces were generated under the same conditions. All experiments involving Brownian data were repeated 100 times with different random seeds.

The results of this experiment are summarized in Tables 1 and 2. The estimates reported in this section are averaged over 100 trials for Brownian data and are the single value for Takagi data. The standard deviation of the estimates for the Brownian data ranged from 0.03 to 0.02.

Tables 1 and 2 suggest that fractal dimension cannot be accurately measured by the naive estimators.

Table 1. Means of naive estimates of fractal dimension on Brownian profiles and surfaces

| $D$ | Variation | Box counting |
|---|---|---|
| 1.1 | 0.99 | 1.21 |
| 1.2 | 1.04 | 1.23 |
| 1.3 | 1.10 | 1.26 |
| 1.4 | 1.17 | 1.29 |
| 1.5 | 1.23 | 1.32 |
| 1.6 | 1.28 | 1.34 |
| 1.7 | 1.33 | 1.36 |
| 1.8 | 1.37 | 1.37 |
| 1.9 | 1.41 | 1.38 |
| 2.1 | 2.26 | 2.07 |
| 2.2 | 2.28 | 2.10 |
| 2.3 | 2.30 | 2.16 |
| 2.4 | 2.32 | 2.22 |
| 2.5 | 2.34 | 2.28 |
| 2.6 | 2.36 | 2.34 |
| 2.7 | 2.37 | 2.38 |
| 2.8 | 2.39 | 2.42 |
| 2.9 | 2.40 | 2.47 |

Table 2. Naive estimates of fractal dimension on Takagi surfaces

| $D$ | Variation | Box counting |
|---|---|---|
| 2.1 | 2.23 | 2.22 |
| 2.2 | 2.27 | 2.25 |
| 2.3 | 2.31 | 2.29 |
| 2.4 | 2.35 | 2.31 |
| 2.5 | 2.40 | 2.34 |
| 2.6 | 2.45 | 2.39 |
| 2.7 | 2.49 | 2.40 |
| 2.8 | 2.54 | 2.38 |
| 2.9 | 2.59 | 2.41 |

Although estimates varied monotonically with fractal dimension, the range of the estimates was much smaller than the range of the "true" dimension and the estimates do not match the true values except at a dimension of about 2.2. Box counting creates a wider range of estimates than the variation method with Brownian data but the reverse is true with Takagi data. The results are disheartening.

The fact that estimators of fractal dimension do not return accurate values on artificial images with known dimensionality has been noted several times in the literature. Keller *et al.*[12] generated ten fractal surfaces by the power spectrum method, having dimensions ranging from 2.0 to 2.9 and estimated dimension with box counting using probabilities. The sizes of the images were not given. Estimated dimensions ranged from 2.07 to 2.53. Their "interpolation method" produced a range from 2.09 to 2.81. They attributed the inaccuracy to the difficulty of sampling surfaces which vary rapidly, as do surfaces with dimension close to 3.0. We call this the resolution effect. Dubuc *et al.*[21] compared the variation estimator and two versions of Peleg *et al.*[15] blanket estimator on Takagi surfaces with true dimension between 2.4 and 2.7 and on fractal Brownian surfaces with true dimension between 2.3 and 2.7. Sample size was not stated. Results were very good, especially for the variation method, with errors below 0.05. However, their ranges of true dimension omit values at which the estimators performed the worst, namely small and large values. In addition, their estimators were optimized in some way and are certainly not "naive" in the sense of this paper.

Log–log plots for the variation and box counting methods on some Takagi surfaces are given in Fig. 3. Those for some Brownian surfaces are given in Fig. 4. The log–log plots are certainly not straight and the data for different values of dimension tend to merge as box size increases. The absence of information about fractal dimension in points corresponding to very small and to very large boxes is apparent.

One might question the validity of the algorithms that generate the data to explain the poor results. Perhaps they do not properly reflect the true fractal dimension. However, these algorithms have been referenced frequently in the literature and the examples in Figs 1 and 2 do agree with intuition. The remainder of this paper investigates other factors which may explain the poor results.

### 5.2. *Optimistic estimators*

The log–log curves in Figs 3 and 4 for 256 × 256 images were re-interpreted to see if any portion of the curve had the "correct" slope. Log–log curves for 512-point profiles were treated in the same manner. Such procedures have no value in practice because they require that the true fractal dimension be known and because the portion of the log–log data used depends on the known fractal dimension. Our objective was to see how the algorithmic parameters vary with fractal dimension and to identify the parameters to which estimates are most sensitive. The results are shown in Tables 3 and 4.

The variation "estimator" computes the slopes of all 5-point segments of the log–log plot and selects the one which best estimates the correct fractal dimension. Such an "optimization" decides at what resolution level the estimate should be computed in order to

Table 3. Means of optimistic estimates of fractal dimension on Brownian profiles and surfaces

| Dimension $D$ | Variation Mean | Variation $k_n^{opt}$ | Box counting Mean | Box counting $l^{opt}$ |
|---|---|---|---|---|
| 1.1 | 1.10 | 4 | 1.09 | 3–6 |
| 1.2 | 1.20 | 6 | 1.20 | 4–6 |
| 1.3 | 1.30 | 11 | 1.28 | 4–7 |
| 1.4 | 1.40 | 21 | 1.39 | 5–7 |
| 1.5 | 1.50 | 33 | 1.48 | 5–8 |
| 1.6 | 1.60 | 53 | 1.61 | 6–8 |
| 1.7 | 1.70 | 91 | 1.69 | 5–9 |
| 1.8 | 1.80 | 176 | 1.80 | 6–9 |
| 1.9 | 1.86 | 231 | 1.94 | 7–9 |
| 2.1 | 2.26 | 2 | 2.09 | 4–6 |
| 2.2 | 2.29 | 2 | 2.19 | 4–7 |
| 2.3 | 2.31 | 2 | 2.30 | 5–7 |
| 2.4 | 2.41 | 3 | 2.37 | 5–7 |
| 2.5 | 2.50 | 5 | 2.56 | 6–7 |
| 2.6 | 2.60 | 11 | 2.61 | 6–7 |
| 2.7 | 2.70 | 31 | 2.70 | 6–7 |
| 2.8 | 2.80 | 76 | 2.79 | 6–7 |
| 2.9 | 2.87 | 124 | 2.90 | 6–7 |

Table. 4. Optimistic estimates of fractal dimension on Takagi surfaces

| True dimension $D$ | Variation Estimate | Variation $k_n^{opt}$ | Box counting Estimate | Box counting $l^{opt}$ |
|---|---|---|---|---|
| 2.1 | 2.22 | 4 | 2.15 | 3–4 |
| 2.2 | 2.26 | 4 | 2.20 | 3–4 |
| 2.3 | 2.31 | 4 | 2.29 | 3–5 |
| 2.4 | 2.39 | 4 | 2.39 | 4–5 |
| 2.5 | 2.50 | 6 | 2.53 | 4–6 |
| 2.6 | 2.59 | 12 | 2.54 | 5–6 |
| 2.7 | 2.68 | 28 | 2.63 | 5–6 |
| 2.8 | 2.81 | 30 | 2.74 | 5–6 |
| 2.9 | 2.90 | 32 | 2.88 | 5–7 |

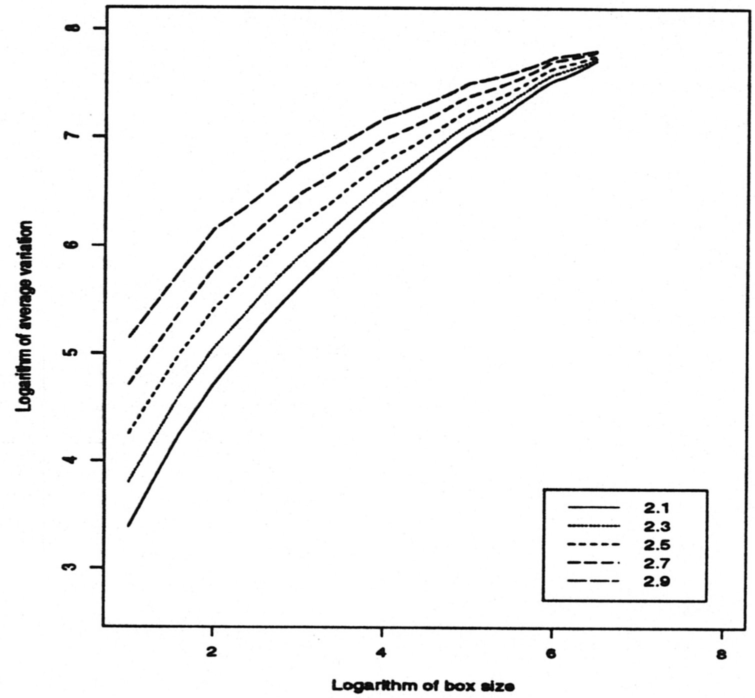


(a)

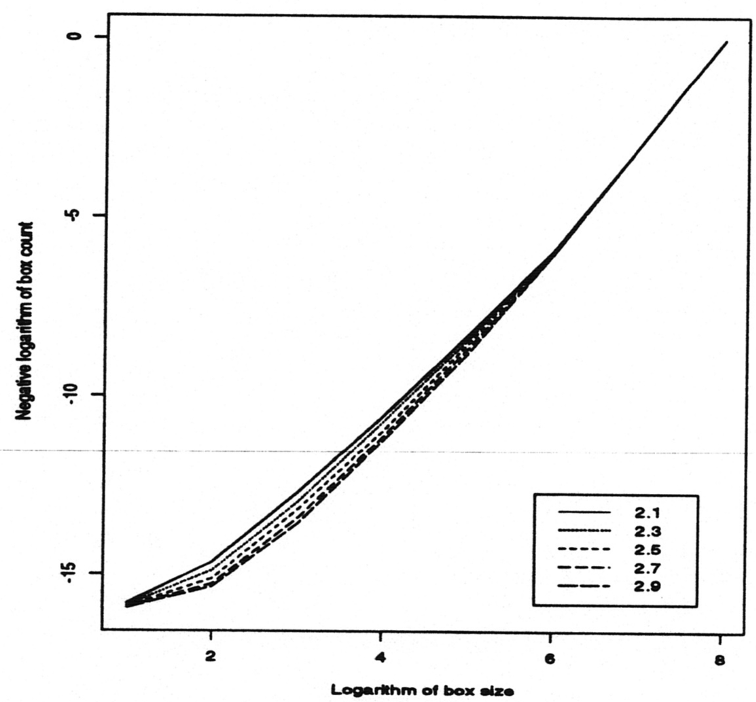


(b)

Fig. 3. Log–log plots with Takagi surfaces of size 256 × 256 from: (a) the variation method; (b) box counting method.

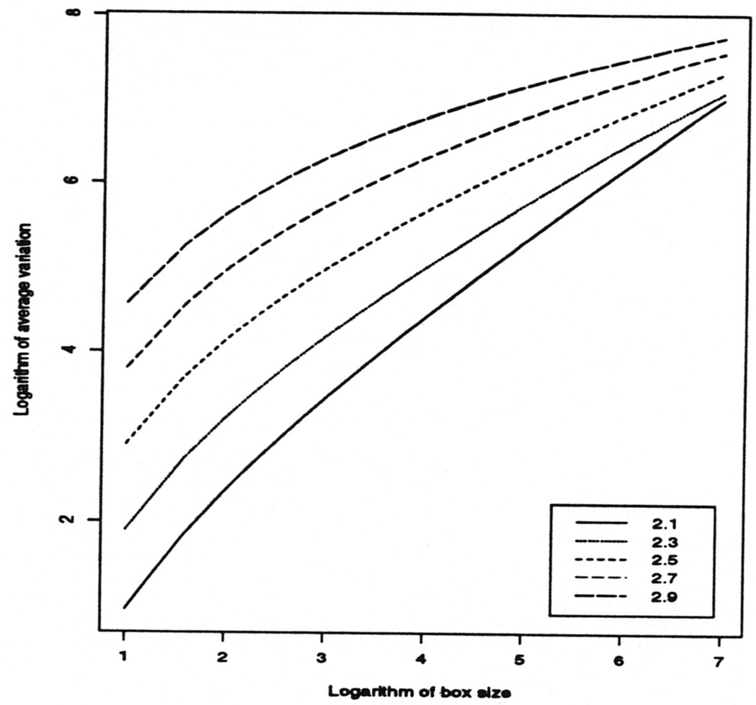


(a)

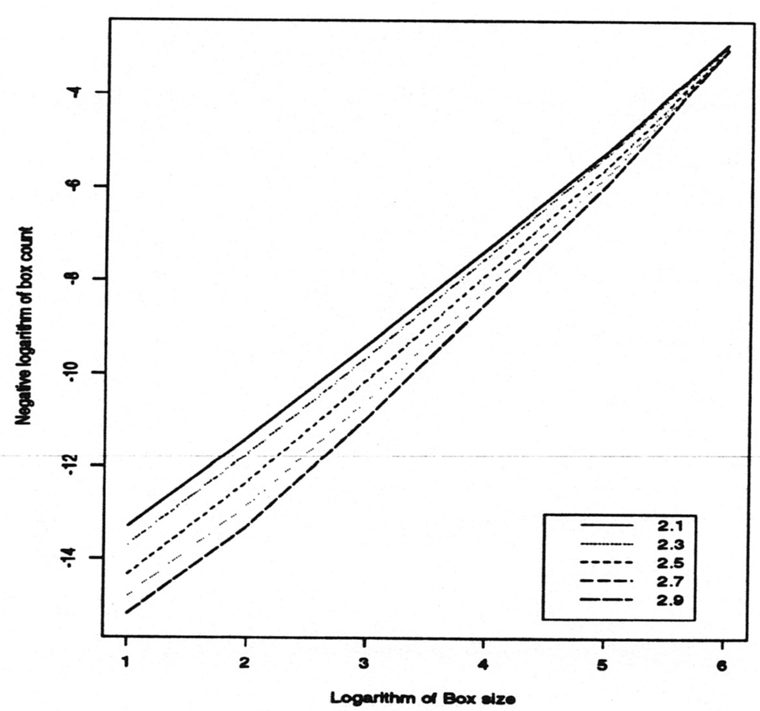


(b)

Fig. 4. Log–log plots with Brownian surfaces of size 256 × 256 from: (a) the variation method; (b) box counting method.

minimize the estimation error. Compared with the practical optimization strategy employed by Dubuc et al.,[20,21] ours also tries to adjust the resolution seen by each box to improve the accuracy of measured oscillation but according to a different criterion. The column labeled $k_n^{opt}$ in Tables 3 and 4 refers to the starting point of the 5-point segment. As dimension increases, one must go further out on the curve (or start at a better resolution level) to get the best estimate. Although the slopes of the log–log curves for large dimension eventually reflected the correct dimension, those for small dimension were often incorrect.

The log–log plots for box counting contain 9 points since $2^9 = 512$ is the largest box size. Slopes were computed for all possible straight lines when choosing the slope closest to the correct dimension value. Column $l^{opt}$ in Tables 3 and 4 lists the ranges of the abscissa. As the dimension increases, only the right-most portion of the log–log plot correctly reflects the dimension. In several cases, only two points were used. The extremes of the log–log plots are not related to fractal dimension, but the value of 9 appears a few times. The optimistic "estimates" are much closer to the true fractal dimension than the estimates in Tables 1 and 2 especially for Brownian curves. The portion of the curve that provides the best estimate is not necessarily the most linear portion of the plot. There is no obvious way of choosing the portion of the plot that yields the "best" estimate.

## 6. RESOLUTION

This section reports on experiments that quantify the effects of resolution on the robustness of fractal dimensionality estimators. Resolution has two components, namely image size and fineness of sampling. Our experiments use mathematical images so these components are related. Mathematically, images are generated in a unit cube, then scaled to an $N \times N \times 256$ rectangular prism. We studied the effects of resolution in two ways. First, we simply vary $N$ and call this resolution varying scheme "resampling". The larger the value of $N$, the higher the resolution since the mathematical image is generated in a unit cube. Second, we averaged small subimages in a given image to produce a smaller, necessarily blurred, image of lower resolution than the given image. We call this process "pyramiding".

In the resampling scheme, the Brownian surfaces were generated in four sizes: 64 × 64, 128 × 128, 256 × 256, and 512 × 512. Pyramided images were formed by starting with a 512 × 512 image and producing smaller ones. The variation method was applied to all Brownian images with the first and the last 10% of points on the log–log plot deleted. Box counting estimators were applied with the first and last points on the log–log plot deleted. All the estimates were averaged over 10 trials. The experimental results for different resolutions using the resampling scheme are shown in Tables 5 and 6. The results from the pyramiding scheme are shown in Tables 7 and 8.

Tables 5 and 6 indicate that better estimates of fractal dimension are obtained as resolution increases when $D$ is greater than 2.5. This result was expected because more samples are available to reflect increased roughness of the fractal surface as $D$ approaches 3.0. Unfortunately, some estimates for small $D$ also increase as resolution increases so the ranges of the estimates are not widened as much as we expected with the improvement of resolution. One explanation for this unexpected performance when $D$ is small lies in our current algorithms. No matter what the resolution, we deleted the same percentage or amount of points from the two ends of log–log plots. Thus, more points on log–log

Table 5. Mean estimates of fractal dimension using the variation method on Brownian surfaces, as functions of $N$

| | Image size | | | |
|---|---|---|---|---|
| Dimension $D$ | 64 × 64 | 128 × 128 | 256 × 256 | 512 × 512 |
| 2.1 | 2.51 | 2.56 | 2.58 | 2.56 |
| 2.3 | 2.52 | 2.62 | 2.62 | 2.66 |
| 2.5 | 2.59 | 2.65 | 2.66 | 2.68 |
| 2.7 | 2.61 | 2.69 | 2.73 | 2.75 |
| 2.9 | 2.68 | 2.72 | 2.77 | 2.80 |

Table 6. Mean estimates of fractal dimension using box counting method on Brownian surfaces, as functions of $N$

| | Image size | | | |
|---|---|---|---|---|
| Dimension $D$ | 64 × 64 | 128 × 128 | 256 × 256 | 512 × 512 |
| 2.1 | 2.42 | 2.42 | 2.41 | 2.39 |
| 2.3 | 2.46 | 2.47 | 2.48 | 2.47 |
| 2.5 | 2.48 | 2.53 | 2.54 | 2.55 |
| 2.7 | 2.47 | 2.56 | 2.60 | 2.62 |
| 2.9 | 2.47 | 2.58 | 2.64 | 2.68 |

Table 7. Mean estimates of fractal dimension using the variation method on Brownian surfaces with pyramiding

| | Image size | | | |
|---|---|---|---|---|
| Dimension $D$ | 64 × 64 | 128 × 128 | 256 × 256 | 512 × 512 |
| 2.1 | 2.44 | 2.48 | 2.52 | 2.55 |
| 2.3 | 2.55 | 2.58 | 2.62 | 2.62 |
| 2.5 | 2.53 | 2.66 | 2.63 | 2.67 |
| 2.7 | 2.59 | 2.64 | 2.69 | 2.73 |
| 2.9 | 2.65 | 2.71 | 2.75 | 2.74 |

Table 8. Mean estimates of fractal dimension using box counting method on Brownian surfaces with pyramiding

| | Image size | | | |
|---|---|---|---|---|
| Dimension $D$ | 64 × 64 | 128 × 128 | 256 × 256 | 512 × 512 |
| 2.1 | 2.37 | 2.42 | 2.42 | 2.39 |
| 2.3 | 2,35 | 2.46 | 2.47 | 2.47 |
| 2.5 | 2.46 | 2.48 | 2.53 | 2.55 |
| 2.7 | 2.44 | 2.51 | 2.57 | 2.62 |
| 2.9 | 2.48 | 2.51 | 2.60 | 2.68 |

plots were actually used for larger resolutions. Therefore, in effect, a second parameter was being varied in addition to resolution. Better assessment of resolution effect may be obtained by scaling the number of points and the portion on the log–log plot according to the resolution. This may benefit the estimates for small $D$ without affecting the positive resolution effect when $D$ is large.

The results in Tables 7 and 8 can be appreciated by noting the drops in mean estimates as the image size decreases. Bigger variations in estimates can be seen for large $D$ than for small $D$ which is expected because the original $512 \times 512$ image is rougher for large $D$ than for small $D$. As in Tables 5 and 6, estimates for small $D$ increase, thus worsen, as resolution increases. The rate at which estimates decrease as resolution decreases is about the same in Tables 7 and 8 as in Tables 5 and 6.

The two approaches to varying resolution, resampling and pyramiding, produced comparable results on both estimators. The observations made under these two schemes seem to re-enforce each other. But, how does resolution affect each estimator differently? Comparing the results from Tables 5 and 7 with that from Tables 6 and 8, the ranges of the estimates from box counting estimator change more consistently toward the correct direction with the increase of resolution. This observation, however, is not significant enough to conclude the difference in resolution effect on the two estimators. Our results here emphasize that practical details of the estimator algorithms can have a dramatic effect on the accuracy of the estimators and simple designed estimators may lead to poor results. Even though we cannot conclude precisely and quantitatively the impact of resolution on the two estimators at the current stage of this study, some estimation scheme based on multiple resolutions could, perhaps, be devised to overcome the resolution effect on estimators of fractal dimension. A different sort of correction to the box counting algorithm for small $D$ was proposed by Taylor and Taylor.[22]

## 7. QUANTIZATION

Images, by their nature, are quantized because each sample is limited to a finite number of gray values. This section examines whether quantization introduces significant error into the variation estimator. It would be meaningless to perform this experiment on the box counting estimator, as it requires quantized data. One hundred Brownian surfaces and the single Tagaki surface, all of size $256 \times 256$, were employed. The slopes of the log–log curves were computed for $k_n$ in the range [8–128] with Takagi surfaces and in the range [14–115] with Brownian surfaces. The results are shown in Tables 9 and 10. Standard deviations were less than 0.1 for Brownian surfaces.

The effect of quantization on Brownian surfaces is clear in Table 10 because the "quantized estimates are about 0.05 smaller than the estimates computed without quantization. The range of estimates is simply shifted. Table 9 indicates a similar effect on Takagi surfaces but with a bigger shift in estimates. Quantized images lead to smaller estimates. This observed effect of quantization is somehow similar to the effect of resolution discussed in Section 6. It is not surprising because quantization is related to resolution. A quantized image is a blurred version of its original non-quantized representation. Quantization and pyramiding blur data in different ways but they yield a similar effect on the performance of the two estimators used in this study.

Table 9. Effect of quantization on the variation method with Takagi surfaces

| $D$ | Non-quantized | Quantized |
|---|---|---|
| 2.1 | 2.64 | 2.46 |
| 2.2 | 2.66 | 2.49 |
| 2.3 | 2.68 | 2.53 |
| 2.4 | 2.71 | 2.56 |
| 2.5 | 2.73 | 2.60 |
| 2.6 | 2.75 | 2.63 |
| 2.7 | 2.78 | 2.67 |
| 2.8 | 2.80 | 2.70 |
| 2.9 | 2.82 | 2.74 |

Table 10. Effect of quantization on the variation method with Brownian surfaces

| $D$ | Non-quantized | Quantized |
|---|---|---|
| 2.1 | 2.22 | 2.16 |
| 2.2 | 2.27 | 2.22 |
| 2.3 | 2.33 | 2.28 |
| 2.4 | 2.40 | 2.37 |
| 2.5 | 2.47 | 2.43 |
| 2.6 | 2.54 | 2.50 |
| 2.7 | 2.60 | 2.57 |
| 2.8 | 2.67 | 2.62 |
| 2.9 | 2.72 | 2.67 |

## 8. CONCLUSIONS

Our study covered a wide range of situations and parameters one may encounter in estimating fractal dimension. The main result is to demonstrate that the parameters of the estimation algorithms and the true values of $D$ significantly affect the accuracy of the estimates. The interaction between the parameters of the estimation algorithms and $D$ may be explained by resolution effect. Naive estimators, which are often practical estimators, are not reliable. Certain optimization seems necessary to improve the quality of estimates, mainly by compensating the resolution effect. The log–log plots from which estimates are computed are not straight, as theory dictates, but information about the "correct" $D$ is somewhere, if only we knew where to look. Trying to find the most linear portion of the log–log curve does not ensure the best estimate.

The poor results for large $D$ can be somewhat overcome by increasing the resolution of sampling but increasing resolution may degrade the estimates for small $D$. The fact that a small $D$ value produces a smooth surface suggests that quantization effects could account for the poor estimates. We cannot claim a definite advantage for either box counting or the variation method. Seeking a better estimator will not remove the inherent difficulties discussed in this paper.

Assuming our generation algorithms are correct, we must conclude that accurate measurement of fractal dimension is difficult on the variety of profiles and images encountered in our experiments. The ranges of the estimates never matched the ranges of $D$ and these ranges were affected by both quantization and resolution. The estimates matched $D$ in only a few cases, usually for $D$ around 2.5. The encouraging conclusion is that the estimates varied monotonically with $D$ so that fractal dimension may be a useful descriptor in image segmentation and texture recognition.

We regret that we cannot completely explain the effects of resolution and quantization on the accuracy of estimators. We would also like to have proposed new and better estimators of fractal dimension. However, we have accomplished our objective of highlighting the difficulties inherent in estimating fractal dimension. The problem is not improper estimators but that the image data do not match the assumptions on which the estimators are based.

*Acknowledgement*—The authors would like to acknowledge the support of the National Science Foundation through grant CDA-8806599.

## REFERENCES

1. B. B. Mandelbrot, *The Fractal Geometry of Nature*. Freeman, New York (1983).
2. H.-O. Peitgen and P. H. Richter, editors, *The Beauty of Fractals*. Springer, New York (1986).
3. T. S. Parker and L. O. Chua, *Practical Numerical Algorithms for Chaotic Systems*. Springer, New York (1989).
4. M. T. Barnsley, *Fractals Everywhere*. Academic Press, New York (1988).
5. M. Fleischmann, D. J. Tildesley and R. C. Ball, editors, *Fractals in the Natural Sciences*. Princeton University Press, Princeton, New Jersey (1989).
6. A. P. Pentland, Fractal-based description of natural scenes, *IEEE Trans. Pattern Analysis Mach. Intell.* **6**(6), 661–674 (1984).
7. C. B. Caldwell, S. J. Stapleton, D. W. Holdsworth, R. A. Jong, W. J. Weiser, G. Cooke and M. J. Yaffe, Characterisation of mammographic parenchymal pattern by fractal dimension, *Phys. Med. Biol.* **35**, 235–247 (1990).
8. P. Kube and A. Pentland, On the imaging of fractal surfaces, *IEEE Trans. Pattern Analysis Mach. Intell.* **10**, 704–707 (1988).
9. A. P. Pentland, Fractal-based description, *Proc. IJCAI*, Karlsruhe, Germany, pp. 973–981, August (1983).
10. C.-C. Chen, J. S. DaPonte and M. D. Fox, Fractal feature analysis and classification in medical imaging, *IEEE Trans. Med. Imaging* **8**, 133–142 (1989).
11. J. Gårding, Properties of fractal intensity surfaces, *Pattern Recognition Lett.* **8**, 319–324 (1988).
12. J. M. Keller, S. Chen and R. M. Crownover, Texture description and segmentation through fractal geometry, *Comput. Vision Graphics Image Process.* **45**, 150–166 (1989).
13. J. M. Keller, R. M. Crownover and R. Y. Chen, Characteristics of natural scenes related to the fractal dimension, *IEEE Trans. Pattern Analysis Mach. Intell.* **9**, 621–627 (1987).
14. P. P. Ohnian and R. C. Dubes, Performance evaluation for four classes of textural features, *Pattern Recognition* (to appear).
15. S. Peleg, J. Naor, R. Hartley and D. Avnir, Multiple resolution texture analysis and classification, *IEEE Trans. Pattern Analysis Mach. Intell.* **6**(4), 518–523 (1984).
16. S. G. Mallat, A theory for multiresolution signal decomposition: the wavelet representation, *IEEE Trans. Pattern Analysis Mach. Intell.* **11**, 674–693 (1989).
17. B. J. Super and A. C. Bovik, Localized measurement of image fractal dimension using Gabor filters, *J. Visual Commun. Image Representation* **2**, 114–128 (1991).
18. J. Theiler, Estimating fractal dimension, *J. Opt. Soc. Am. A* **7**, 1055–1073 (1990).
19. K. Falconer, *Fractal Geometry, Mathematical Foundations and Applications*. Wiley, New York (1990).
20. B. Dubuc, J. F. Quiniou, C. Roques-Carmes, C. Tricot and S. W. Zucker, Evaluating the fractal dimension of profiles, *Phys. Rev. A* **39**, 1500–1512 (1989).
21. B. Dubuc, S. W. Zucker, C. Tricott, J. F. Quiniou and D. Wehbi, Evaluating the fractal dimension of surfaces, *Proc. R. Soc. London A* **425**, 113–127 (1989).
22. C. C. Taylor and S. J. Taylor, Estimating the dimension of a fractal, *J. R. Statist. Soc. Ser. B* **533**, 353–364 (1991).
23. C. D. Cutler and D. A. Dawson, Estimation of dimension for spatially distributed data and related limit theorems, *J. Multivariate Analysis* **28**, 115–148 (1989).
24. Y. Ogata and K. Katsura, Maximum likelihood estimates of the fractal dimension for random spatial patterns, *Biometrika* **78**, 463–474 (1991).
25. N. Sarkar and B. B. Chaudhuri, An efficient approach to estimate fractal dimension of textural images, *Pattern Recognition* **25**, 1035–1041 (1992).
26. L. S. Liebovitch and T. Toth, A fast algorithm to determine fractal dimensions by box counting, *Phys. Lett. A* **141**, 386–390 (1989).
27. R. Voss, Random fractals: characterization and measurement, *Scaling Phenomena in Disordered Systems*, R. Pynn and A. Skjeltorp, eds, pp. 1–11. Plenum Press, New York (1986).
28. H.-O. Peitgen and D. Saupe, editors, *The Science of Fractal Images*. Springer, New York (1988).

**About the Author**—QIAN HUANG was born in Shanghai, China. She received the B.S. degree in computer engineering from Shanghai University of Technology, a graduate student at Jiao Tong University, and the M.S. degree in computer science from Kansas State University. She is currently a Ph.D. candidate in the Computer Science Department at Michigan State University, East Lansing. Qian Huang is a member of IEEE, Phi Kappa Phi, Epsilon Pi Epsilon, and Phi Beta Delta.

**About the Author**—JACOB R. LORCH was born in Washington, D.C. He received the B.S. degree in computer science and the B.S. degree in mathematics from Michigan State University in 1992. He is a National Science Foundation Fellow pursuing a Ph.D. in computer science at the University of California at Berkeley.

**About the Author**—RICHARD C. DUBES was born in Chicago, Illinois. He received the B.S. degree from the University of Illinois and the M.S. and Ph.D. degrees from Michigan State University in 1959 and 1962, respectively, all in electrical engineering. He is a professor in the Computer Science Department at Michigan State University, East Lansing, and is a member of the Pattern Recognition Society, a senior member of IEEE, and Past-president of the Classification Society.